Numerical Methods in Civil Engineering

Journal Homepage: https://nmce.kntu.ac.ir/

Seismic risk-based optimal design of fluid viscous dampers for seismically excited nonlinear structures

Mohtasham Mohebbi* **and Sina Bakhshinezhad****

Abstract:

This paper introduces a procedure to risk-based optimal design of fluid viscous dampers (FVDs). To this end, the exceedance probability of specific performance level during the design lifetime as a safety criterion of the entire building is intended to be minimized. This, along with the minimization of the total damping coefficient of FVDs as the cost criterion of the dissipation system, are the considered objective functions. The damping coefficient of FVDs have been considered as design variables and the efficient configurations of damper properties over the height of the building have been determined. A multi-objective optimization framework using the non-dominated sorting genetic algorithm version II (NSGA-II) has been employed to solve the optimization problems and determine the set of Pareto optimal solutions. Linear and nonlinear FVDs with different capacities have been designed for an eight-story shear-type building with bilinear elastic-plastic stiffness behavior under 20 real earthquakes. The results show that the optimal FVDs reduce the seismic response and fragility of the building, while limiting the dampers' cost.

1. Introduction

Among the natural hazards, earthquakes pose a threat to buildings and bridges and can cause severe losses and casualties. In recent years many studies focused on mitigating the earthquake consequences by using innovative methods. To this end, several novel structural protective systems have been proposed and developed to the level of practical implementation. The structural protective methods can be classified into three main categories: (1) Seismic isolation systems, (2) Passive energy dissipation systems, and (3) Active and semi-active systems. Particularly, passive energy dissipation devices have the advantages of not requiring external power sources and feasible installation to retrofit the existing buildings.

The fluid viscous dampers (FVDs) have appeared as a highly efficient energy dissipation system in reducing structural seismic demands.

The effectiveness of these passive dampers has been demonstrated through different applications such as installation in bracing systems, base isolation systems, and tuned mass dampers and prompted more attention by researchers [1-4] and producers [5,6]. Several design methods of FVDs have been developed considering their distribution over the height of building and implementation costs. De Domenico et al. [7] have presented a brief review of the fundamentals of most of these methods. Although several methodologies have proposed optimal design of FVDs for seismically excited buildings, the key shortcoming of these methodologies is that they do not explicitly consider the uncertainties in earthquake excitation. Thus, they cannot directly control the seismic hazard risk and may not always yield a reliable design for the dampers.

* *Corresponding author: Professor, Faculty of Engineering, University of Mohaghegh Ardabili , Ardabil, Iran. Email: Mohebbi@uma.ac.ir*
** *PhD, Faculty of Engineering, University of Mohaghegh Ardabili, Ardabil, Iran.*

More recent studies have demonstrated the effects of application of fluid viscous damper in a probabilistic framework [8-13]. Despite the importance of a probabilistic approach to design energy dissipation devices, few studies have addressed this issue which can be used to mitigate the seismic risk of buildings equipped with dampers. Shu et al. [14] have designed pendulum tuned mass damper systems for a coal-fired power plant building using performance-based analysis. Different values for the parameters of this device have been considered and optimum values have been detected such that the direct loss is minimized. Radu et al. [15] have designed a tuned inerter damper that was installed between the base and first floor of a five-story structure. The performance of the system has been defined based on the probability distribution function of the top story displacement. Altieri et al. [16] have designed viscous dampers for a 3-story steel building using an optimization technique incorporating constraint on structural performance. The damper cost, which depends on the damper forces, has been considered as an objective function, and the constraint on the probability of exceedance of specific performance levels has been taken into account. In the light of these studies, designing FVDs considering the seismic risk of building as a control objective has not been accomplished previously.

This study proposes a methodology for seismic risk-based optimal design of fluid viscous dampers for seismically excited buildings. To this end, the exceedance probability of the specific performance level during the design lifetime has been evaluated according to the performance-based earthquake engineering (PBEE) framework [17] and defined as one objective function. Further, the total damping coefficient of FVDs as the cost criterion of the dissipation system has also been considered as an alternate objective function. Since these objective functions conflict with each other, an efficient multi-objective optimization procedure has been employed to design linear and nonlinear FVDs for a sample case study building.

The rest of the paper is organized as follows: in section 2, the formulation of PBEE framework to quantify the seismic risk of the seismically excited structure is described; in section 3, the equations of motion of the nonlinear structure equipped with fluid viscous dampers is presented; in section 4, the risk-based optimal design methodology using multi-objective optimization is explained; in section 5, the proposed method is applied to design fluid viscous dampers for a case study consisting of a nonlinear eight-story shear building frame, followed by discussion and conclusion.

2. Risk formulation based on PEER PBEE framework

The Performance-based earthquake engineering, PBEE, framework is a general probabilistic approach for the performance assessment and design of structures subjected to seismic hazards which has been proposed at the PEER center [17]. The framework incorporates the following four probabilistic analysis steps: (1) probabilistic seismic hazards analysis, which characterizes the uncertainty of the input excitation intensity measures (IMs); (2) probabilistic seismic demand analysis; which represents uncertain estimates of engineering demand parameters (EDPs) conditional on the IMs (3); probabilistic seismic damage analysis, denoting the uncertainty of damage measures (DMs) or damage states; and (4) probabilistic seismic loss analysis, which presents the uncertainty of the decision variable (DV). The PEER framework equation expresses the mean annual frequency (MAF) of exceedance of a decision variable as:

$$\lambda(dv) = \int_{dm}\int_{edp}\int_{im} G(dv|dm).\left|dG(dm|edp)\right|$$
$$.\left|dG(edp|im)\right|.\left|d\lambda(im)\right| \tag{1}$$

For IM, EDP, DM, and DV, upper case letters signify random variables and lower case letters denote specific realizations. $G(x|y)=P(x<X|Y=y)$ denotes the complementary (joint) cumulative distribution function of variable X conditional on Y=y. $\lambda(im)$ denotes the MAF of an intensity measure which can be described by Eq. (2) by assuming that the occurrence of significant earthquakes follows a Poisson process.

$$\lambda(IM) = 1-\exp[-(IM/u)^{-k}] \approx (IM/u)^{-k}$$
$$= k_0 IM^{-k} \text{ (at large values of IM)} \tag{2}$$

in which u is the scale parameter, k is shape parameter, and constant $k_0=u^k$. The performance-based procedure developed in this study requires the MAF of exceedance of specified damage states. Thus, only the first three steps of the framework are involved. This MAF can be expressed as:

$$\lambda(dm) = \int_{edp}\int_{im} G(dm|edp).\left|dG(edp|im)\right|.\left|d\lambda(im)\right| \tag{3}$$

An important intermediate result of PBEE framework is the probability of exceedance of the considered damage states conditional on the intensity measure which is commonly called the fragility curve in the literature and is as follows:

$$P(dm|im) = \int_{edp} G(dm|edp).\left|dG(edp|im)\right| \tag{4}$$

Finally, assuming that a Poisson process can describe the failure occurrence of the system, the value of failure probability during the design lifetime, *t*, can be evaluated as:

$$P_{f,t} = 1 - \exp[-\lambda(dm).t] \qquad (5)$$

This failure probability has been considered as an objective function to design FVDs. Actually, the first three performance evaluation steps of the PEER framework is required in this procedure. However, the life cycle cost could also be considered as the design objective which entails taking into account the full performance evaluation steps of the PEER framework.

2.1 Closed-form solution

To estimate the uncertain EDP, a relation between intensity measure and seismic demand of the structure should be established. In this regard, incremental dynamic analysis is a common approach that is based on scaling the set of ground motions to a specific IM and increasing them until the desired damage state is reached. However, this method may alter the frequency content of the earthquake records due to scaling. This limitation could be resolved by using the power model proposed by Cornell et al. [18] according to Equation (6) which is widely employed in many performance assessment studies concerning the structural control systems similar to those considered in this work [19-21]. In this procedure, only, the dynamic analysis at the original scale of earthquakes is required and therefore, a drastic reduction in computational costs is produced.

$$EDP = a.IM^b \qquad (6)$$

where *a* and *b* are model constants that could be evaluated by performing a linear regression analysis of ln(*EDP*) on ln(*IM*). The demand uncertainty or dispersion is obtained by:

$$\beta_{EDP|IM} = \sqrt{\ln(1 + S^2)} \qquad (7)$$

in which S^2 is the standard error as:

$$S^2 = \sum \left(\ln(edp_i) - \ln(edp_p) \right) / n - 2 \qquad (8)$$

where edp_i and edp_p are the observed and predicted demand of the structure, respectively, and n is the number of response sample data. Under the assumption that the seismic demand, EDP, and the capacity of the structural

system, DM, follow the lognormal distribution, Equations (3) and (4) can be reformulated as follows [18]:

$$\lambda(dm) = k_0 \left(IM^{DM} \right)^{-k} . \exp\left[\frac{1}{2} \frac{k^2}{b^2} \left(\beta_{EDP|IM}^2 + \beta_{DM}^2 \right) \right] \qquad (9)$$

$$P(dm|im) = \Phi\left[\frac{\ln(EDP) - \ln(DM)}{\sqrt{\beta_{EDP|IM}^2 + \beta_{DM}^2}} \right] \qquad (10)$$

in which IM^{DM} is the corresponding ground motion intensities to the *DM* based on inverting the power model of Equation (6) [18]. Φ denotes the standard normal cumulative distribution function. The damage measure terms, *DM* and β_{DM}, depend on the performance level of interest and have been addressed in the next sub-section.

2.2 Capacity and uncertainty of damage states

The evaluation of the reliability of a structure equipped with a control system requires selecting proper damage states that are related to the performance of the entire structure. Regarding the whole structure, the inter-story drift ratio (IDR) has been adopted as a global EDP which correlates with the damage of structural components as a safety criterion. Analogous to FEMA 356 [22], capacity thresholds for inter-story drift ratio associated with steel moment frames have been selected as the values of 0.7%, 2.5% and 5% related to Immediate Occupancy (IO), Life Safety (LS) and Collapse Prevention (CP) performance levels, respectively. It is noteworthy that to explain that for the procedure of performance-based design of the FVDs, the IO performance level has been considered for the case study of this research as an example. Also, this procedure could be applied for other performance levels, if satisfying another performance level is necessary. The capacity uncertainty has been selected as the value of 0.25 for IO performance level following [21].
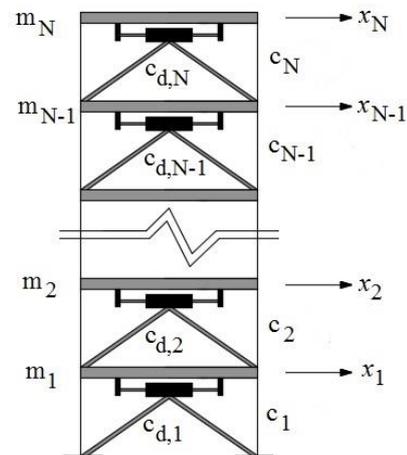

Fig. 1: Schematic of FVD-structure model

3. Motion equation of the structure equipped with FVD

Fig. 1 schematically shows the *N* story shear building structure equipped with FVDs installed between all successive floors. The dampers are installed in a horizontal position by chevron bracings. In this figure, *m* and *c* are the mass and damping coefficients of the building. c_d is the damping coefficient of the damper and *x* is the displacement with respect to the ground.

The equation of motion of this shear-type building with nonlinear behaviour under ground acceleration $\ddot{x}_g$ is as follows:

$$\mathbf{M}\ddot{x}(t) + \mathbf{f}_D\left(\dot{x}(t)\right) + \mathbf{f}_S\left(\mathbf{x}(t)\right) = \mathbf{D}\mathbf{f}_d(t) + \mathbf{M}\mathbf{e}\ddot{x}_g(t) \quad (11)$$

where $\mathbf{x} = [x_1, x_2, \ldots, x_N]^T$, $\dot{\mathbf{x}} = [\dot{x}_1, \dot{x}_2, \ldots, \dot{x}_N]^T$, and $\ddot{\mathbf{x}} = [\ddot{x}_1, \ddot{x}_2, \ldots, \ddot{x}_N]^T$ are respectively the displacement, velocity, and acceleration vectors with respect to the ground. The vector $\mathbf{e} = [-1, \ldots, -1]^T$ denotes the ground acceleration-mass transformation vector. The diagonal mass matrix is as:

$$\mathbf{M} = \begin{bmatrix} m_1 & 0 & L & 0 \\ 0 & m_2 & L & 0 \\ M & M & O & M \\ 0 & 0 & L & m_N \end{bmatrix} \quad (12)$$

By assuming a linear behaviour for the force-velocity of the building, the damping force vector could be written as:

$$\mathbf{f}_D\left(\dot{x}(t)\right) = \mathbf{C}\dot{x}(t) \quad (13)$$

where the damping matrix of the structure, **C**, is defined as:

$$\mathbf{C} = \begin{bmatrix} c_1+c_2 & -c_2 & L & 0 & 0 \\ -c_2 & c_2+c_3 & L & 0 & 0 \\ M & M & O & M & M \\ 0 & 0 & L & c_{N-1}+c_N & -c_N \\ 0 & 0 & L & -c_N & c_N \end{bmatrix} \quad (14)$$

in which c_i denotes the damping coefficient of the *i*-th story. The restoring force vector, $\mathbf{F}_S$, is a function of displacement response of the building. It should be noted that the building even controlled by energy dissipation devices may undergo nonlinear behaviour under seismic excitations and thus the nonlinearity of the structural behaviour should be accounted for. To this end, the force-displacement relationship should be defined to evaluate the restoring force at each time step. It is assumed that the structural stiffness model is consistent on bilinear

hysteretic behaviour as shown in Fig. 2, which is described by the elastic stiffness K_E, post-elastic stiffness K_{PE}, and yielding drift u_y.

D is the location matrix of FVDs assuming to be installed in a horizontal position in all stories as:

$$\mathbf{D} = \begin{bmatrix} -1 & 1 & L & 0 & 0 \\ 0 & -1 & L & 0 & 0 \\ M & O & O & M & M \\ 0 & 0 & O & -1 & 1 \\ 0 & 0 & L & 0 & -1 \end{bmatrix} \quad (15)$$
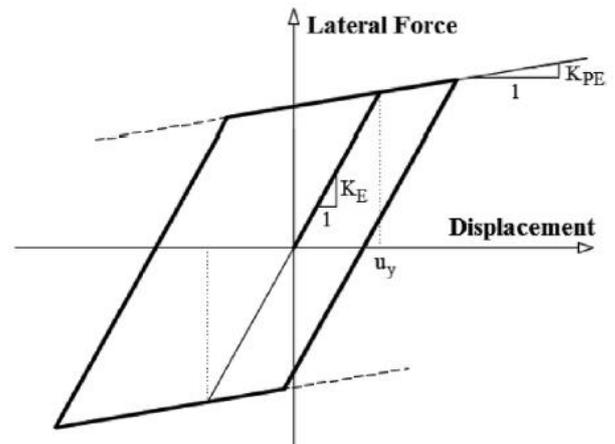

Fig. 2: Bilinear elastic-plastic stiffness model

$\mathbf{f}_d = [f_{d,1}, f_{d,2}, \ldots, f_{d,N}]^T$ is the vector of FVDs control force applied to the successive floors of the structures which can be expressed as follows:

$$f_{d,i}(t) = c_{d,i} v_i^n(t) \qquad i = 1, 2, \ldots, N \quad (16)$$

in which v_i is the relative velocity of the two ends of the *i*-th damper and $c_{d,i}$ is the damping coefficient of the *i*-th damper. The velocity exponent of the damper is shown by *n* and relates to the passing quality of the fluid. The velocity exponent is usually between 0.15 and 1 in structural engineering applications [3], and describes the linear or nonlinear behaviour of FVDs. The linear FVD has the velocity exponent equal to *n*=1, while the nonlinear FVD has the velocity exponent lower than one (*n*<1). In this study, FVDs with both linear and nonlinear behaviour have been designed for the building. For the nonlinear FVDs different values of *n*=0.6, 0.3 and 0.15 have been considered. It should be noted that increasing the nonlinearity level of FVDs causes a remarkable reduction in damper force, and thus in manufacturing cost.

4. Risk-based optimal design method

This section describes the proposed method to risk-based optimal design of the FVDs using an optimization

technique. This method incorporates two main phases including the risk analysis to determine the exceedance probability of specific performance level during lifetime (inner loop) and optimization process (outer loop).

4.1 Risk analysis based on PBEE framework

The direct solution of the risk-based optimal design problem entails performing a full performance analysis for each individual in optimization iterations. This process has been described in the following steps and Fig. 3.

Step 1: Select a set of real probable earthquake records with different characteristics for the region that the structure is located in

Step 2: Consider the site hazard properties including shape parameter, k, and scale parameter, k_0, according to Equation (2) for the site of interest.

Step 3: Conduct nonlinear dynamic analysis for the structure equipped with FVD system and determine maximum IDR subjected to each earthquake by solving the equation of motion of the structure presented in Equation (11).

Step 4: Perform regression analysis to determine the parameters of the power model, a and b, according to Equation (6) and calculate demand uncertainties, $\beta_{IDR|IM}$, according to Equation (7).

Step 5: Consider the capacity thresholds and the related uncertainties for the IDR damage state according to sub-section 2.2.

Step 6: Calculate the probability of exceedance of the specific performance level during the design lifetime based on Equation (5).
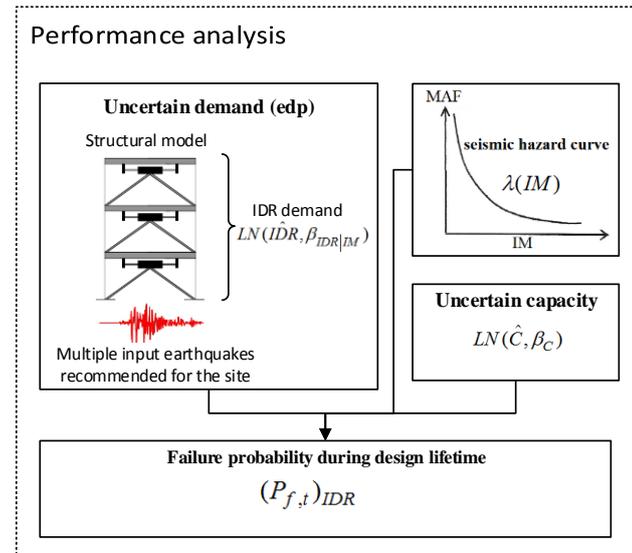

Fig. 3: Description of the subset risk analysis of risk-based optimal design method

It should be noted that the maximum IDR has been employed to risk-based optimal design in this paper following FEMA 356 [22] guidelines. Moreover, the

maximum absolute acceleration of the building as a criterion of occupants' convenience and safety of non-structural components has been considered for risk-based assessment of the controlled buildings previously [23]. However, to focus on the main subject of this research which has been risk-based optimal design of FVDs, in this paper the maximum IDR has been used as design criterion and the performance evaluation considering absolute acceleration has been neglected in the present work, while this limitation could be resolved in further studies by considering both the maximum IDR and absolute acceleration in risk-based design procedure.

4.2 Optimization process

In the optimization phase, the probability of exceedance of the specific performance level during the design lifetime has been used as the objective function to be minimized. Indeed, the probabilistic performance of the structure is involved directly in design process of the FVD system to ensure a reliable design. As mentioned before, the maximum IDR response of the entire structure has been considered as the performance criterion, which is a safety criterion of the structural components. Alongside, regarding the cost criterion, the reduction in manufacturing cost of the damper has been widely intended in most of the previous studies on designing FVD systems. The manufacturing cost is a function of damper force and pro-type testing [24]. Also, the total damping coefficient of dampers is an approximate estimate of initial cost of the FVDs. This quantity has been considered extensively as the objective function or constraint in optimization based procedures of designing FVDs in the literature [25, 26]. Hence, limiting the total damping coefficient of FVDs can reduce the cost of the control system and is desired in the design process. Therefore, in this paper, the following two objective functions have been considered: (1) minimization of the exceedance probability of the specific performance level during the design lifetime and (2) minimization of the total damping coefficient of the FVDs. These objective functions for designing FVD system are in conflict with each other. Solving such a problem entails the utilization of multi-objective optimization, which represents a set of optimal solutions known as Pareto front. Generally, the multi-objective optimization problem could be defined as:

$$
\begin{aligned}
&\textit{Find}: &&\mathbf{X}^* = [X_1^*, X_2^*, ..., X_n^*]^T \\
&\textit{Optimize}: &&\mathbf{f}(\mathbf{X}) = [f_1(\mathbf{X}), f_2(\mathbf{X}), ..., f_m(\mathbf{X})]^T \\
&\textit{Subject to}: &&g_i(\mathbf{X}) \geq 0, \quad i = 1, 2, ..., q \\
& &&h_j(\mathbf{X}) = 0, \quad j = 1, 2, ..., r
\end{aligned} \tag{17}
$$

in which, $\mathbf{X}$ is the vector of design variables that may have several solutions, $\mathbf{X}^*$, to optimize the objective functions. $\mathbf{f}$

denotes the vector of *m* objective functions. *g* and *h* are respectively *q* inequality and *r* equality constraints which should be satisfied. The multi-objective optimization problem for designing the FVDs with the aforementioned objective functions and the design variables of dampers' damping coefficients is formulated as follows:

$$
\begin{aligned}
Find: \quad & c_{d,1}, c_{d,2}, ..., c_{d,i} \quad (i = 1, 2, ..., N) \\
Minimize: \quad & f_1 = P_{f,t} \\
& f_2 = \sum_{i=1}^{N} c_{d,i} \\
Subject\ to: \quad & c_{d,\min} \leq c_{d,i} \leq c_{d,\max}
\end{aligned}
\tag{18}
$$

where *N* is the number of stories and $c_{d,i}$ denotes the damping coefficient of the *i*-th fluid viscous damper. Also, $c_{d,min}$ and $c_{d,max}$ are respectively the minimum and maximum damping coefficient of the dampers that can be considered as construction constraints and are determined by the manufacturer.

4.3 Optimization using NSGA-II

Several metaheuristic algorithms have been introduced to solve the optimization problems in the scientific and industrial fields [27-29]. Genetic algorithm (GA) [30] is one of the most capable methods among several optimization methods and is effective for solving nonlinear optimization problems even with many design variables. This optimization method has been extensively employed in the field of civil engineering [31-33] as well as designing energy dissipation devices [34-36] and has three main operations including selection, crossover, and mutation [37].

A multi-objective optimization problem could be converted to single objective problems and could be solved by classical optimization methods. However, several runs with different adjustments are required. Accordingly, different multi-objective optimization algorithms have been developed to solve these problems in a single run. The non-dominated sorting genetic algorithm (NSGA) [38] was more efficient in solving such problems. Further, the improved versions of this algorithm including NSGA-II [39] and NSGA-III [40] have been proposed.

For the problem at hand with two objective functions and a few design variables, the NSGA-II still seems proper and has been employed for solving the multi-objective optimization problem, as employed for designing dissipation devices previously [41]. The proposed multi-objective optimal design of FVDs based on NSGA-II algorithm is shown in Fig. 4. This algorithm incorporates nine operations including: Initialization, fitness evaluation, non-dominated sorting, crowding distance calculation,

selection, crossover, mutation, combination, and truncate. The readers are recommended to see [41] for more details of this algorithm.
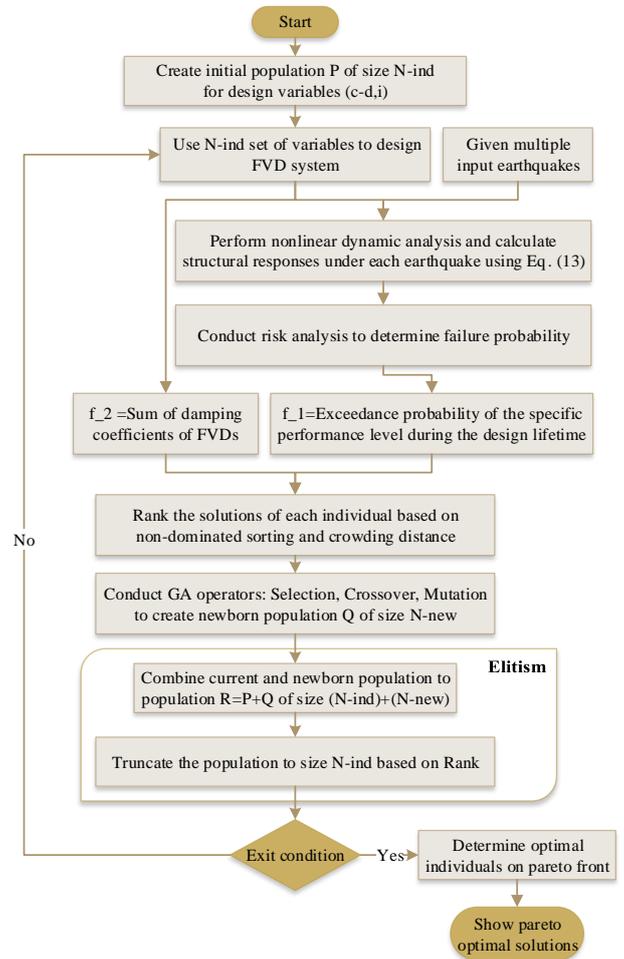

Fig. 4: Flowchart for multi-objective optimal design of FVD system based on NSGA-II algorithm

5. Numerical analysis and discussion

In this section, the methodology of risk-based optimal design of FVD systems for nonlinear structures has been explained through numerical analysis. The objectives of minimization of exceedance probability of the specific performance level during the design lifetime and total damping coefficient of FVDs have been considered in a bi-objective optimization problem. The NSGA-II method has been utilized to solve the optimization problem and design of FVD systems with linear and nonlinear behavior. The FVDs installed in each story of an eight-story nonlinear shear building frame with bilinear hysteretic model is shown in Fig. 2. The structural properties are identical in building height. The mass and damping coefficient are respectively m=345.6 ton and c=734.3 kN.s/m. The height of each story is 3.2 m. The elastic stiffness, post-elastic stiffness, and yielding drift are K_E=3.404×10^5 kN/m,

K_{PE}=3.404×10⁴ kN/m, and u_y=2.4 cm, respectively. The fundamental period of the building is T_1=1.087 sec considering the elastic stiffness. It should be noted that the other sources of uncertainties such as building and damper properties can affect the probabilistic performance of the controlled structure [42]. However, for the preliminary design of FVDs only the uncertainty of earthquake excitation can be more important in the risk-based optimal design method.

5.1 Earthquake ground motions set used in this study

To account for record-to-record variability [43], it is more appropriate to select a set of different earthquakes with different characteristics for the performance assessment of seismic structures. The application of 7 pairs of earthquakes would be sufficient to accurately estimate the structural responses [44]. A set of 10 pairs of earthquakes with the probability occurrence of 10% in 50 years proposed for SAC project for Los Angeles area have been used for performance analysis. These earthquakes have different frequency contents, intensities and duration to represent the variability of the seismic source. The characteristics of the selected ground motion records have been presented in Table 1. Fig. 5 shows the acceleration response spectrum of the selected earthquakes and the mean spectrum for 5% critical damping. As mentioned in sub-section 4.1, the estimation of the exceedance probability of a specific performance level requires descriptions of the seismic hazard. For the Los Angeles area, the region of interest in this study, the shape parameter is k=2.69 and the constant is k_0=1.66×10⁻⁴ [21].

Table. 1: Selected earthquakes records used in this study

| Earthquake code	Earthquake name	Station	PGA (g)
La01	Imperial Valley-f_n	El Centro	0.46
La02	Imperial Valley-f_p	El Centro	0.68
La03	Imperial Valley-f_n	Array #05	0.39
La04	Imperial Valley-f_p	Array #05	0.49
La05	Imperial Valley-f_n	Array #06	0.30
La06	Imperial Valley-f_p	Array #06	0.23
La07	Landers-f_n	Barstow	0.42
La08	Landers-f_p	Barstow	0.43
La09	Landers-f_n	Yermo	0.52
La10	Landers-f_p	Yermo	0.36
La11	Loma Prieta-f_n	Gilroy	0.67
La12	Loma Prieta-f_p	Gilroy	0.97
La13	Northridge-f_n	Newhall	0.68
La14	Northridge-f_p	Newhall	0.66
La15	Northridge-f_n	Rinaldi RS	0.53
La16	Northridge-f_p	Rinaldi RS	0.58
La17	Northridge-f_n	Sylmar	0.57
La18	Northridge-f_p	Sylmar	0.82
La19	North Palm Springs-f_n	-	1.02
La20	North Palm Springs-f_p	-	0.99
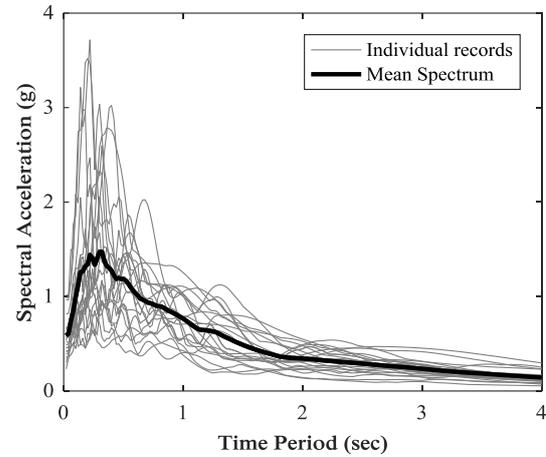
Fig. 5: Acceleration response spectrum of the selected earthquake records and the mean acceleration response spectrum

5.2 Risk-based optimal design of FVD system using NSGA-II

In this section, the fluid viscous dampers with linear and nonlinear behaviour installed on successive floors have been designed for the nonlinear building through solving multi-objective optimization problems using NSGA-II method. The probability of exceedance of different performance levels during the lifetime of the uncontrolled reference building are about 67.03%, 2.89% and 0.34% respectively at IO, LS and CP performance levels. As this value is remarkable only for IO performance level here, it has been focused on FVD design for this performance level. Note that the minimum and maximum damping coefficient of the dampers, $c_{d,min}$ and $c_{d,max}$, should be selected considering the FVDs manufacturers' constraints. These values have been selected equal to 0 and 20,000 kN.s/m according to Moradpour and Dehestani [3]. The optimization algorithm is adjusted such that it searches for design variables within this pre-defined boundary and therefore satisfies the constraints in Equation (18). For different values of velocity exponent regarding linear (n=1) and nonlinear (n=0.6, 0.3, 0.15) FVDs, the optimization problem defined in Equation (18) has been solved frequently by NSGA-II. The parameters of the NSGA-II have been selected as reported in Table 2. To ensure the accuracy of the optimization method, at least four different simulation runs of NSGA-II with different initial random populations have been performed for the optimization problems.

The Pareto optimal solutions related to linear FVDs with the maximum force capacity of F_{max}=1000 kN for four different simulation runs are shown in Fig. 6. It is observed that the Pareto fronts of different runs stand almost close to

each other, which offers several optimal solutions for the FVD system. Compared with the uncontrolled case, the optimal FVDs have shown the capability to reduce the exceedance probability of the IO performance level during the lifetime close to 14%, as compared to 67% for the uncontrolled building.
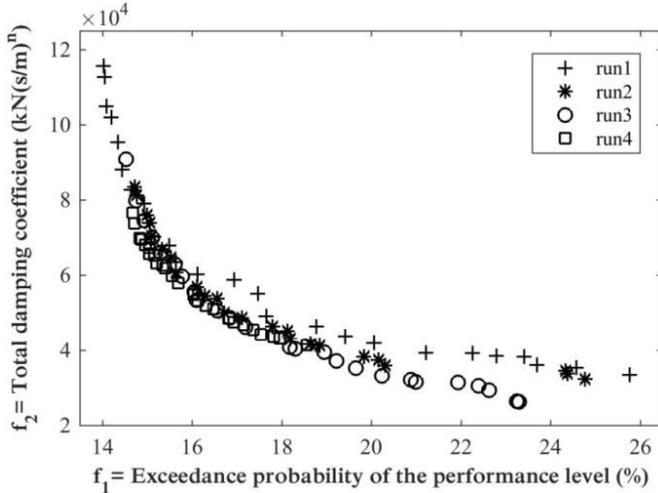

Fig. 6: Pareto fronts of linear FVDs with F_{max}=1000 kN

Table. 2: Parameters of NSGA-II method

N_{ind}	Number of individuals in each generation	25
N_{New}	Number of newborns	18
m_r	Mutation rate	0.02
N_{max}	Maximum number of generation	50

Fig. 7 shows the Pareto fronts correspond to linear FVDs with velocity exponent n=1as well as nonlinear FVDs with velocity exponent n=0.6, 0.3, and 0.15 with the maximum force capacity of F_{max}=1000 kN. It should be noted that the damping coefficients for different velocity exponents have different units and are not directly comparable. However, it seems that nonlinear FVDs can also reduce seismic hazard risk of the building significantly. In particular, linear FVDs with velocity exponent of n=0.3 decreased the exceedance probability of the IO performance level during the lifetime close to 12%. As an example, linear FVDs require a total damping coefficient of 6.75×10^4 kN(s/m) to provide an exceedance probability of 15%, while the nonlinear FVDs with n=0.3 enables this level of risk enhancement by total damping coefficient of 2×10^4 kN(s/m)^n.
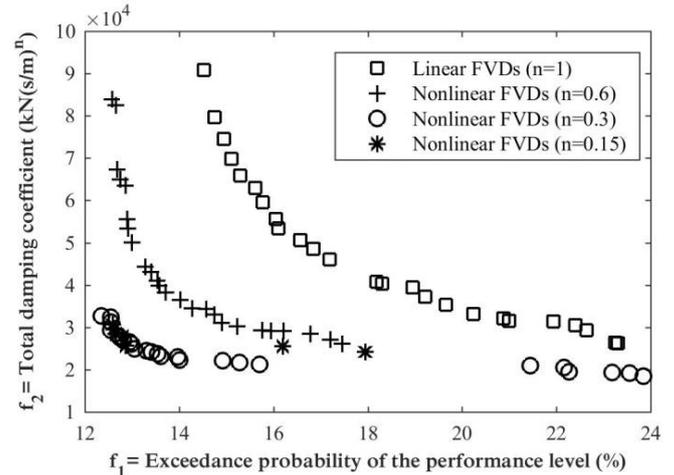

Fig. 7: Pareto fronts of linear and nonlinear FVDs

Along with the total damping coefficient, the damper force capacity heavily affects the manufacturing cost of the FVDs and has been defined as design objective in some studies [16]. In this research, although the maximum damper force has not directly minimized, some pre-defined values have been considered for this property. The pre-defined values of maximum damper force includes F_{max}=500, 750, 1000, and 1500 kN. The proposed method has been applied to design FVDs with different capacities and the resulted Pareto fronts for linear FVDs are illustrated in Fig. 8. It is observed that higher damper force capacity has led to more mitigation in risk of the building.

5.3 Probabilistic performance of FVDs designed by the risk-based optimal design method

In this section, the probabilistic performance of the linear and nonlinear FVDs designed by the risk-based optimal design method has been assessed and compared with that of uncontrolled structure. As shown in the previous section, the Pareto fronts contain several optimal solutions for the designed FVDs. In this section, one optimal solution has been selected for each of the linear and nonlinear FVDs and has been used to control the structural responses. As a sample, the solution related to the total damping coefficient of 3×10^4 kN.s/m is selected. This total damping coefficient corresponds to the exceedance probability of the IO performance level during the lifetime as approximately equal to 22.4%, 15.8%, and 12.6% respectively for linear FVD (n=1), and nonlinear FVD with n=0.6 and n=0.3, as can be seen in Fig. 7. Table 3 reports the optimal damping coefficients of each floor for linear and nonlinear FVDs.

Table. 3: *Optimal damping coefficients of linear and nonlinear FVDs*

Story number	Optimal damping coefficients kN(s/m)^n		
	n=1	n=0.6	n=0.3
1	9370.4	7967.2	10020.4
2	4360.6	4670.9	3314.6
3	5479.6	5916.9	3265.7

4	2120.0	3006.3	3148.04
5	5344.5	3221.0	4094.4
6	2541.1	2863.6	3000.8
7	796.2	443.0	3853.0
8	536.4	1284.8	554.2

For the sake of comparison, a simplified procedure proposed in FEMA 356 [22] and discussed in [7] has been used to design FVDs with uniform distribution over the building's height. To this end, the total damping of 3×10^4 kN.s/m, similar to those selected for the optimal dampers, has been considered for the uniform distributed (UD) FVDs. The mean responses under 20 earthquakes for the building equipped with optimal FVDs and UD FVDs have been compared with that of uncontrolled building in Table 4. Also, the reductions of these responses with respect to the uncontrolled building have been compared in this table. It seems that the optimal FVDs have the capability of reducing the maximum IDR and absolute acceleration responses with respect to the uncontrolled structure. Also, from the results it is clear that using optimal FVDs has resulted in a slightly greater reduction in the maximum IDR compared to UD FVDs. The IDR response reduction as a safety criterion is enhanced by increasing the nonlinearity level of the FVDs. However, this effect for acceleration response is vice versa and the linear FVD has reduced the acceleration response more effectively. It should be noted that this study has focused on IDR demand by following FEMA356 [22] guidelines and other seismic demands such as acceleration as a convenience criterion, can be of interest in further studies. The fragility curves of the uncontrolled building as well as the building equipped with linear and nonlinear optimal and UD FVDs have been developed using Equation (10) and compared in Fig. 9. It can be observed that the optimal FVDs can reasonably reduce the seismic fragility of the building. The FVDs with nonlinear behaviour (n=0.3) have mitigated the fragility slightly more than the other FVDs.
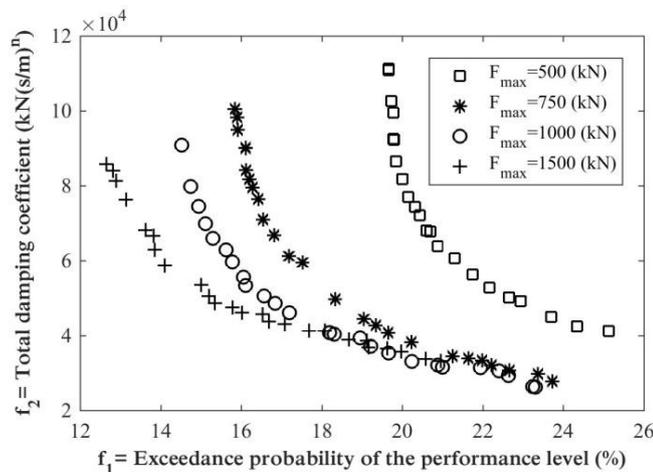

Fig. 8: Pareto fronts of the linear FVDs with different force capacities

Table 4: *The mean responses under 20 earthquakes*

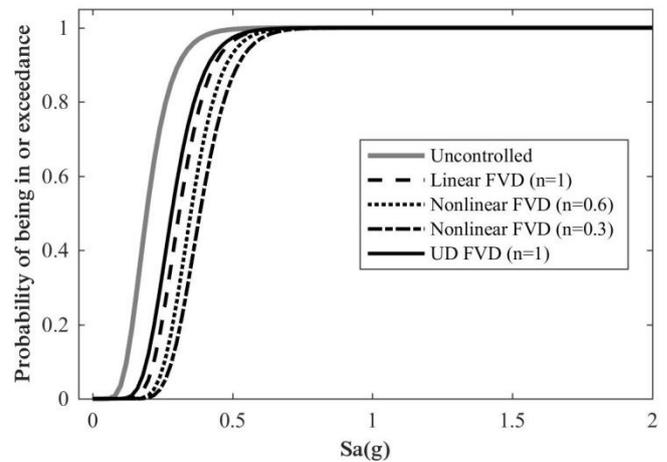| Mechanism	Maximum IDR	Maximum absolute acceleration (cm/s²)	Reduction with respect to uncontrolled (%)	
			IDR	acceleration
Uncontrolled	0.0237	1191	-	-
Linear FVD (n=1)	0.0192	896	19	25
Nonlinear FVD (n=0.6)	0.0194	921	18	23
Nonlinear FVD (n=0.3)	0.0185	1120	22	6
UD FVD (n=1)	0.020	841	16	32

Fig. 9: Fragility curves of the uncontrolled building and the building equipped with linear and nonlinear optimal FVDs

6. Conclusions

In this study, the aim is to present a methodology for risk-based optimal design of fluid viscous damper for seismically excited nonlinear structures to account for earthquake uncertainty. The exceedance probability of the specific performance level during the design lifetime as a safety criterion as well as the total damping coefficient of FVDs as the cost criterion have been considered as objective functions. The damping coefficients of FVDs over the height of the building have been considered as design variables. A multi-objective optimization problem has been defined and solved using non-dominated sorting genetic algorithm version II (NSGA-II). For illustration, the method has been applied to design linear and nonlinear FVDs for an eight-story shear-type building with hysteretic bilinear elastic-plastic behaviour subjected to 20 real earthquakes. The results of numerical simulations have shown that the capability and simplicity of the applied method which provides several optimal solutions minimizes both the seismic hazard risk of the building and dampers' costs simultaneously throughout the Pareto

fronts. It has been shown that the optimal FVDs can reduce the exceedance probability of the performance level during the lifetime to almost 12%, which was conversely 67% for the uncontrolled building. Comparing the linear and nonlinear FVDs shows that nonlinear FVDs require approximately lower total damping coefficient than linear FVDs to limit the exceedance probability of the performance level during the lifetime. As an example, nonlinear FVDs with velocity exponent n=0.3 require the total damping coefficient of 2×10^4 kN(s/m)^n to limit the exceedance probability of IO performance level to 15%, while the linear FVDs need the total damping coefficient of 6.75×10^4 kN(s/m) to this level of seismic risk enhancement. Besides, the probabilistic performance of the designed linear and nonlinear FVDs have been assessed and compared through developing fragility curves. It is observed that the designed FVD systems can reasonably enhance the seismic fragility with respect to the uncontrolled building.

References:

[1] Shariati A, Kamgar R, Rahgozar R. Optimum layout nonlinear fluid viscous damper for improvement the response of tall buildings, *Int J Optim Civil Eng* 2020; **10**(3): 411-431.

[2] Hashemi MR, Vahdani R, Gerami M, Kheyrodin A. Viscous damper placement optimization in concrete structures using colliding bodies algorithm and story damage index, *Int J Optim Civil Eng* 2020; **10**(1): 57-70.

[3] Moradpour S, Dehestani M. Optimal DDBD procedure for designing steel structures with nonlinear fluid viscous dampers, *Struct* 2019; **22**: 154-174.

[4] Idels O, Lavan O. Optimization-based seismic design of steel moment-resisting frames with nonlinear viscous dampers, *Struct Control Health Monit* 2020; **28**(1): e2655.

[5] Taylor, Taylor Devices Inc, https://www.taylordevices.com/.

[6] Tensa, Tensa Gruppo De Eccher, https://www.tensacciai.it/

[7] De Domenico, Ricciardi G, Takewaki I. Design strategies of viscous dampers for seismic protection of building structures: A review, *Soil Dyn Earthq Eng* 2019; **118**(Mar) 144-165.

[8] Di paola M, La Mendola L, Navarra G. Stochastic seismic analysis of structures with nonlinear viscous dampers, *J Struct Eng* 2007; **133**(10): 1475-1478.

[9] Tubaldi E, Barbato M, DallAsta A. Performance-based seismic risk assessment for buildings equipped with linear and nonlinear viscous dampers, *Eng Struct* 2014; **78**: 90-99.

[10] Dall'Asta A, Tubaldi E, Ragni L. Influence of the nonlinear behavior of viscous dampers on the seismic demand hazard of building frames, *Earthq Eng Struct Dyn* 2016; **45**(1): 149-169.

[11] Guneyisi EM, Altay G. Seismic fragility assessment of effectiveness of viscous dampers in R/C buildings under scenario earthquakes, *Struct Saf* 2008; **30**(5): 461-480.

[12] Lavan O, Avishur M. Seismic behavior of viscously damped yielding frames under structural and damping uncertainties, *Bull Earthq Eng* 2013; **11**(6): 2309-2332.

[13] Dall'Asta A, Scozzese F, Ragni L, Tubaldi E. Effect of the damper property variability on the seismic reliability of systems equipped with viscous dampers. *Bull Earthq Eng* 2017; **15**: 5025-5053.

[14] Shu Z, Li S, Sun X, He M. Performance-based seismic design of a pendulum tuned mass damper system, *J Earthq Eng* 2019; **23**(2): 334-355.

[15] Radu A, Lazar IF, Neild SA. Performance-based seismic design of tuned inerter dampers, *Struct Control Health Monit* 2019; **26**(5): e2346.

[16] Altieri D, Tubaldi E, Angelis MD, Patelli E, Dall'Asta A. Reliability-based optimal design of nonlinear viscous dampers for the seismic protection of structural systems, *Bull Earthq Eng* 2018; **16**(2): 963-982.

[17] Kiureghian AD. Non-ergodicity and PEER's framework formula, *Earthq Eng Struct Dynamics* 2005; **34**(13): 1643-1652.

[18] Cornell CA, Jalayer F, Hamburger RO, Foutch DA. Probabilistic basis for 2000 SAC federal emergency management agency steel moment frame guidelines, *J Struct Eng* 2002; **128**(4): 526-533.

[19] Bakhshinezhad S, Mohebbi M. Multiple failure function based fragility curves for structures equipped with TMD, *Earthq End Eng Vib* 2021; **20**(2): 471-482.

[20] Bakhshinezhad S, Mohebbi M. Fragility curves for structures equipped with optimal SATMDs, *Int J Optim Civil Eng* 2019; **9**(3): 437-455.

[21] Ellingwood BR, Kinali K. Quantifying and communicating uncertainty in seismic risk assessment, *Struct Saf* 2009; 31(2): 179-187.

[22] FEMA 356. Prestandard and commentary for the seismic rehabilitation of buildings prepared by the American Society of Civil Engineers for the Federal Emergency Management Agency, Washington, D.C, 2000.

[23] Mohebbi M, Bakhshinezhad S. Multiple performance criteria-based risk assessment for structures equipped with MR dampers, *Earthq Struct* 2021; **20**(5): 495-512.

[24] Pollini N, Lavan O, Amir O. Optimization-based minimum-cost seismic retrofitting of hysteretic frames with nonlinear fluid viscous dampers, *Earth Eng Struct Dyn* 2018; **47**(15): 2985–3005.

[25] De Domenico D, Ricciardi G. Earthquake protection of structures with nonlinear viscous dampers optimized through an energy-based stochastic approach, *Eng Struct* 2019; **179**: 523-539.

[26] Aydin E, Öztürk B, Dutkiewicz M. Analysis of efficiency of passive dampers in multistorey buildings, *J Sound Vib* 2019; **439**: 17-28.

[27] Shabani A, Asgarian B, Salido M. Search and rescue optimization algorithm for size optimization of truss structures with discrete variables, *Int J Numer Methods Civil Eng* 2019; **3**(3): 28-39.

[28] Shabani A, Asgarian B, Salido M, Gharebaghi SA. Search and rescue optimization algorithm: A new optimization method for solving constrained engineering optimization problems, *Expert Systems with Applications* 2020; **161**: 113698.

[29] Shabani A, Asgarian B, Salido M, Gharebaghi SA, Salido MA, Giret A. A new optimization algorithm based on search

and rescue operations, *Mathematical Problems in Engineering* 2019.

[30] Holland JH. *Adaptation in Natural and Artificial Systems*, Ann Arbor: The University of Michigan Press, 1975.

[31] Moradi M, Bagherieh AR, Esfahani MR. Damage and plasticity of conventional and high-strength concrete part1: statistical optimization using genetic algorithm, *Int J Optim Civil Eng* 2018; **8**(1): 77-99.

[32] Gholizadeh S, Kamyab R, Dadashi H. Performance-based design optimization of steel moment frames, *Int J Optim Civil Eng* 2013; **3**(2): 327-43.

[33] Biabani Hamedani K, Kalatjari VR. Structural system reliability-based optimization of truss structures using genetic algorithm, *Int J Optim Civil Eng* 2018; **8**(4): 565-86.

[34] Mohebbi M, Moradpour S, Ghanbarpour Y. Improving the seismic behavior of nonlinear steel structures using optimal MTMDs, *Int J Optim Civil Eng* 2014; **4**(1): 137-50.

[35] Mohebbi M, Bagherkhani A. Optimal design of Magneto-Rheological Dampers, *Int J Optim Civil Eng* 2014; **4**(3): 361-80.

[36] Mohebbi M, Dadkhah H. Optimal smart isolation system for multiple earthquakes, *Int J Optim Civil Eng* 2019; **9**(1): 19-37.

[37] Goldberg DE. *Genetic Algorithms in Search, Optimization and Machine Learning*, Reading MA: Addison-Wesley, 1989.

[38] Srinivas N, Deb K. Multiobjective optimization using nondominated sorting in genetic algorithms, *Evol Comput* 1994; **2**(3): 221-248.

[39] Deb K, Pratap A, Agarwal S, Meyarivan T. A fast and elitist multiobjective genetic algorithm: NSGA-II, *IEEE T Evolut Comput* 2002; **6**(2): 182-197.

[40] Deb K, Jain H. An evolutionary many-objective optimization algorithm using reference-point-based nondominated sorting approach, Part I: Solving problems with box constraints, *IEEE T Evolut Comput* 2014; **18**(4): 577-601.

[41] Bakhshinezhad S, Mohebbi M. Multi-objective optimal design of semi-active fluid viscous dampers for nonlinear structures using NSGA-II, *Struct* 2020; 24: 678-689.

[42] Bakhshinezhad S, Mohebbi M. Multiple failure criteria-based fragility curves for structures equipped with SATMDs, *Earthq Struct* 2019; **17**(5): 463-475.

[43] Iervolino I, Cornell CA. Record selection for nonlinear seismic analysis of structures, *Earthq Spectra* 2005; **21**(3): 685-713.

[44] Kiani J, Camp C, Pezeshk S. On the number of required response history analyses, *Bull Earthq Eng* 2018; **16**: 5195-5226.